2

SPRAY DROPLET SOURCE FUNCTION: FROM LABORATORY TO OPEN SEA

Gerritt de Leeuw
TNO Physics and Electronics Laboratory,
P.O. Box 96864, 2509 JG The Hague, The Netherlands

1. INTRODUCTION

A comprehensive model for the fate and influence of the aerosol in the marine atmospheric boundary layer (MABL) requires, among others, a precise consideration of the sources and sinks. These include the exchange of aerosol at the air-sea interface and at the top of the boundary layer, shrinking and growing of the aerosol in a varying field of relative humidity, and advection. Obviously, these processes influence not only the concentrations in the MABL, but also the shapes of the aerosol profiles. The latter is the subject of this paper, where we discuss source functions in relation to profiles of large droplets (radius r>5 μm) near the air-sea interface. Droplet profiles measured over the ocean will be reviewed and compared with droplet profiles measured during CLUSE-HEXIST laboratory experiments. Common features and differences are highlighted. An attempt will be made to explain the weaker concentration gradients near the sea surface. This is based on consideration of surface production of jet droplets from rising air bubbles and entrainment of 'aged' aerosol from the well mixed boundary layer into the surface layer. A sea spray droplet source function will be derived, based on a review of oceanic and laboratory bubble spectra.

2. AEROSOL PROFILES

2.1 Oceanic aerosol profiles

Droplet concentration profiles (radius r>5 μm) measured over the North Atlantic in 1983 in high wind speeds (U>7 m/s) show minima close to the sea surface and maxima at levels near the wave crests, which become more obvious as wind speed increases [De Leeuw, 1986]. The minimum was ascribed to the limited ejection height of the droplets [De Leeuw, 1986; Wu, 1990]. The maximum was conjectured to be due to the action of a wave rotor caused by flow separation on the breaking waves [De Leeuw, 1986; 1990b]. The occurrence of

minima and maxima in the droplet concentration profiles was confirmed by the measurements made over the North Sea in high winds during the HEXOS Pilot Experiment in the Fall of 1984 at Meetpost Noordwijk (MPN), 10 km from the Dutch coast [De Leeuw, 1987].

A comprehensive data set was collected during the HEXMAX experiments which took place at MPN in the Fall of 1986. During HEXMAX two different physical principles were applied to detect the particles:

- an impaction method using the Rotorod sampler which was also employed during the 1983 and 1984 experiments
- detection of laser light scattered by droplets passing through a small sample volume [De Leeuw et al., 1990].

Both methods yield similar results, and the occurrence of minima and maxima in the droplet concentration profiles was observed with both methods. However, in many other cases with high wind speeds these features were not observed [De Leeuw, 1990a]. This shows that effects other than flow separation (e.g., turbulence) may be important as well.

The occurrence of competing processes apparently causes either a minimum-maximum profile shape or profiles without such a distinct structure. Comprehensive discussions of the various processes which may affect the profile shapes have been presented in De Leeuw [1990a, b]. To decide which of these processes are really important, numerical calculations are required which take each of these into account [De Leeuw, 1989]. A first attempt along these lines to investigate the importance of a reverse air flow in the wave troughs is presented in Edson and De Leeuw [1990].

A common feature of the droplet concentration profiles near the ocean surface is that the observed gradients are weaker than expected (cf. De Leeuw [1988]). Strong gradients were predicted, e.g., by Blanchard and Woodcock [1980] based on data collected at different locations in different meteorological conditions with different methods. Models based on surface layer similarity [Fairall and Davidson, 1986], K-diffusion [Stramska, 1987; Rouault et al., 1990], or Lagrangian trajectory calculations [Edson, 1989] also predict strong surface gradients. The profiles predicted by the CLUSE models [Edson, 1989; Rouault et al., 1990] compare favourably with laboratory data.

2.2 CLUSE-HEXIST aerosol profiles

During the CLUSE-HEXIST laboratory experiments, very strong gradients have been observed near the surface [Mestayer et al., 1987; Edson, 1989; Rouault et al., 1990]. The droplet concentrations decreased by 1-2 orders of magnitude when the sampling height was increased from 0.12 m to 0.65 m above the water surface. These experiments were made in the Large Air-Sea Interaction Simulation Tunnel (IMST, Luminy, Marseille), where droplets were produced from bubbles created when air was forced through a mesh of ceramic aerators submerged at 50 cm below the fresh water surface. During the HEXIST experiments a 0.6m x 1m bubbler net was used to simulate a single whitecap, which enables measurement of, e.g., advection of the aerosol. To enhance the effect of the aerosol on atmospheric water vapor and temperature profiles, a 100% whitecap was simulated during the GRAND-CLUSE experiments (May-June 1988) by submerging aerators over a length of 30 m, from the entrance of the tunnel to the samplers. The aerosol produced as jet and film droplets from the bursting bubbles was advected by the wind and dispersed in the vertical by the

turbulence created by the friction at the air water interface. Wind speed and temperatures (air, water and dew point) could be adjusted independently.

2.3 Differences between CLUSE and oceanic aerosol profiles

The aerosol created at the tunnel air-water interface consists of fresh water droplets which evaporate completely when the dew point is lower than the air temperature. Other effective removal mechanisms are provided by the tunnel heat exchangers, which remove the moisture from the return air flow, and by the ventilators and other surfaces in the return flow channel which may remove the aerosol by impaction. Therefore, the only source of large droplets in the tunnel is the production by the bursting bubbles. These freshly produced droplets add to the circulating background aerosol consisting of fine hygroscopic dust particles [Mestayer et al., 1987].

Over the ocean, on the other hand, advection and mixing are important. The concentrations of the long-living small and intermediate size particles forming the 'background' aerosol are mainly determined by advection. As an example, the Navy Aerosol Model (for latest version see Gathman [1989]) discerns four modes. Three of these, the non-hygroscopic and hygroscopic small-particle modes and the 'aged' marine mode consisting of particles of intermediate size, are produced elsewhere. For the largest sea-spray droplets the advection terms are usually neglected because of their short residence time. These droplets can be considered well-mixed at the levels where they are generally measured (10 m). Once they reach levels higher than the wave tops they have a good chance to be transported over many wave periods before they are deposited.

Very close to the surface the well-mixed assumption will not apply because the aerosol production is discontinuous or intermittent (this is further discussed in section 3). Calculations by Stramska [1987], using a mean source function, show that it takes many hours to achieve a quasi-stationary state: The response times of the aerosol to changes in the surface production rate varies from 0.5 hours for 15 μm radius particles, to 28 hours for 0.5 μm particles, which is much longer than the response to changes in the boundary layer properties [Fairall et al., 1983]. Hence, in a field with relatively high concentrations, the short-term variations of the production rate go unnoticed, unless perhaps when measurements are made in the region where the freshly produced droplets are ejected, i.e., before they are mixed with the particles falling from the well-mixed region. Wu et al. [1984] observed patches of large ($r>25$ μm) droplets at 0.3 and 0.5 m, which were ascribed to local production near the crests. De Leeuw [1989] observed fluctuations in the concentrations of smaller droplets which correlate with the motion of the underlying water surface. Results from the HEXIST experiments and Lagrangian model calculations [Mestayer and Lefauconnier, 1987; Mestayer et al., 1987] show that the concentrations of jet droplets generated from a 'bubbler' point source vary strongly as a function of the distance from the source.

This leads to the following picture. The aerosol in the boundary-layer is effectively a reservoir from which particles are continuously entrained into the surface layer due to gravitation. Consequently, the aerosol concentration near the sea surface are determined by the sum of the aerosol concentration in the boundary layer and the rate of production at the surface. The strong gradients of the freshly produced droplets near the sea surface, which are

conjectured to be similar to the gradients observed in laboratory experiments, contribute to the observed profile, but they do not determine the shape due to the mixing with the aged aerosol which has accumulated to much higher concentrations than the freshly produced droplets.

2.4 Laboratory sea-water experiments: Petit-CLUSE 3 and 4

The Petit-CLUSE 3 and 4 (PCL3 and PCL4) sea-water experiments in the UCONN whitecap simulation tank can in some respects be regarded as intermediate between the fresh water experiments in the IMST tunnel and field experiments over the ocean. During the PCL3 and PCL4 experiments the aerosol was produced by bubbles generated from a 1m x 1m aerator grid, which was further identical to the one used during GRAND-CLUSE. Mixing in the tank was achieved by a clean-air flow through the hood of the tank, and by a set of four ventilators mounted at the four sides of the hood.

Considerably different aerosol spectra were observed when the tank was filled with fresh water or with sea water. The concentrations were much higher over sea water. This results from two effects:

- with the same flow rate through the bubblers, the fresh water bubbles are larger, and their concentrations lower, than those in sea water. These two effects result in a lower surface production rate in fresh water as compared to sea water.
- the fresh water droplets evaporate completely, whereas the residual sea salt aerosol accumulates in the tank.

During PCL3, sea salt aerosol profiles were measured with the Rotorod impaction samplers at levels between 0.015 m and 0.08 m, with a resolution of 0.0045 m. At higher levels some samples were obtained as well. The initial analysis shows that the effects of the residual sea salt droplets on the profiles can be observed when profiles measured over the region where the bubbles burst are compared with profiles measured at the side of the bubble patch, and by comparison between profiles measured with the tank opened or closed. With the tank open, much of the aerosol appeared to be efficiently removed from the tank, while also the relative humidity was low and mixing properties were strongly affected. The sum of these effects cause strongly decreasing concentrations of the larger ($r>28$ μm) droplets in the lower 0.1 m over the bubble patch, see Figure 1. The (negative) gradients decrease with increasing droplet size. For droplets with $r<20$ μm the concentrations are rather uniform in the lowest 0.1 m and in fact decrease slightly below 0.03 m. The cause of the latter effect is not obvious, but it may be an indication that the concentrations of the smaller droplets increase at higher levels due to evaporation of larger ones, while deposition near the surface is enhanced due to the decrease in resistance caused by the broken surface over the bubble patch [Larsen et al., 1990] or due to scavenging by the freshly produced droplets. The latter may be an effective process over the continuous bubble patch in the tank because of the high production rate of film droplets (up to 1000 for the largest bubbles [Blanchard, 1983]) having a large horizontal velocity component. In addition, the surface flux hardly contributes to the near-surface concentrations because the ejection velocities are too high.

With the hood down the gradients near the surface are weaker, and the concentrations above 0.04-0.05 m are more uniform and much higher than with the hood up. At the side of the bubble patch the concentrations are similar to

those observed at the higher levels over the bubble patch, indicating that the droplets are well mixed throughout the tank. The aerosol is uniformly distributed over the lower 10 cm at the side of the bubble patch.

The PCL3 data illustrate both the effect of surface production and removal on the observed profiles and the effect of the residual sea salt aerosol. In particular, the similarity of the concentrations over the bubble patch at levels above the influence of direct production and the concentrations beside the bubble patch shows that the profiles are to a large extent determined by the well-mixed residual sea salt component.

For over-ocean conditions this implies that the concentrations near the surface are determined by those in the well-mixed layer, and modified by processes occurring near the air-sea interface. This is in agreement with the observed shapes of oceanic profiles discussed in section 2. The influence of the surface production is only observed at the lowest levels. For estimating the surface source function from particle size distributions measured at 10 m these effects should be taken into account.

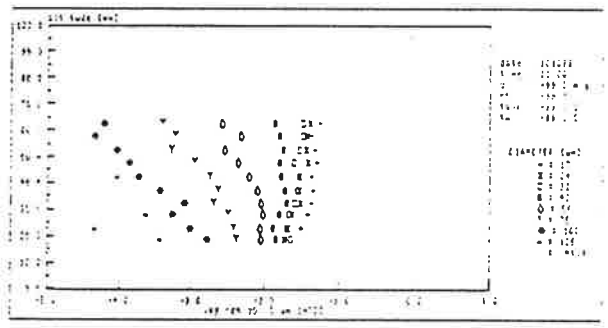

Figure 1. Droplet profiles measured during PCL3 over sea water from 0.02 to 0.065 m, hood up.

3. AEROSOL PRODUCTION AT THE SURFACE

Very few attempts have been made to determine the surface source functions for the marine aerosol, see Miller and Fairall [1988] for a review. The budget method was used by Toba [1965], to derive the source function from data measured by Woodcock [1953] at cloud base from the balance between surface production and gravitational fallout. Fairall et al. [1983] included entrainment at the top of the mixed-layer and subsidence in the balance equation and applied this to field data recorded during an extended period with steady wind speeds of 9 m/s. Surface fluxes for other wind speeds were subsequently obtained. The same model was applied to derive surface source functions from NAM-estimated aerosol concentrations [Miller and Fairall, 1988]. Monahan et al. [1983] determined a source function from the oceanic whitecap coverage and the production rate per unit whitecap area determined from laboratory experiments. This method neglects vertical mixing due to turbulence, which results in discrepancies for the larger (>5 μm) particles. Based on their review, Miller and Fairall [1988] proposed a consensus source function, see Figure 3. During the CLUSE experiments the source functions were obtained by Edson [1989] based on various assumptions on the bubble spectrum

and resulting jet droplet flux. His results compare favourably with the droplet source function derived by De Leeuw [unpublished results] from the upward flux of the freshly produced droplets, which was directly measured with MgO-coated glass slides.

3.1 Bubble spectra

Marine aerosols are produced from bubbles bursting at the surface and, at high wind speeds, by direct tearing from the crests. The discussion in this paper will be limited to bubble-mediated aerosol production. Bubbles are formed when waves break, due to the entrainment of air in the water. The bubbles are entrained to depths of several meters and rise to the surface due to buoyancy. Wu [1990] derived a surface source function from extrapolation of bubble spectra measured by Kolovayev [1976] and by Johnson and Cooke [1979], with photographic methods at several depths and wind speeds. This analysis requires some comments on both the extrapolation to zero depth and on the size dependence. An expression for the exponential variation with depth, $N/N_o=\exp(z/z_b)$, was obtained from consideration of the total number of bubbles N (cf. Wu [1981]), which is determined by only a small part of the bubble spectrum. We feel that fundamentally it is more correct to consider bubble spectra rather than total bubble concentrations. The data in Figure 2 of Wu [1981] show that the total number concentrations of the bubbles obtained from Johnson and Cooke's spectra decrease faster with depth than those derived from Kolovayev's data. Our analysis of the depth dependence of the Johnson and Cooke spectra yields profiles which are similar for all sizes, with an average characteristic length scale z_b of 1 m. The analysis of Kolovayev's 1.5 and 4 m data, on the other hand, shows a systematic variation of the characteristic length scale with bubble size (the omission of the 8 m data is justified because below 4 m the logarithmic bubble profiles change to power law profiles). For bubbles with radii R smaller than about 100 μm an average characteristic length scale of 1.4 m was obtained. For greater bubbles this scale decreases gradually to 0.8 m for 200 μm bubbles. The characteristic length scale for bubbles larger than 200 μm averages around 1 m. The characteristic length scale presented in Wu [1989], $z_b=0.4+0.12(U_{10}-7)$ for $U_{10}>7$ m/s, is derived from a fit to Thorpe's [1982] cross sections for acoustic scattering at various wind speeds, which is forced through the characteristic length scale given in Wu [1981] (1 m at 12 m/s).

The size dependence used by Wu [1989] is a power law: $N(R)\sim R^{-4}$. In his initial analysis, Wu obtained powers of -3.5 from Kolovayev's results and -5 from the Johnson and Cooke data [Wu, 1981]. Apparently Wu [1988, 1989] values Kolovayev's data higher as regards the size dependence, whereas for the depth dependence he prefers the data of Johnson and Cooke.

In Figure 2 we compare the surface droplet spectrum given by Wu [1989] with the spectra obtained from our extrapolation of the data of Kolovayev [1976] and Johnson and Cooke [1979], with acoustic data presented in Medwin and Breitz [1989] (their Figure 6) and the bubble spectrum obtained by Monahan [1988] from backward analysis of the Monahan et al. [1986] source function. Wu's spectrum, which contains a proportionality factor for the size dependence, was adjusted to match the extrapolated Johnson and Cooke data around 100 μm.

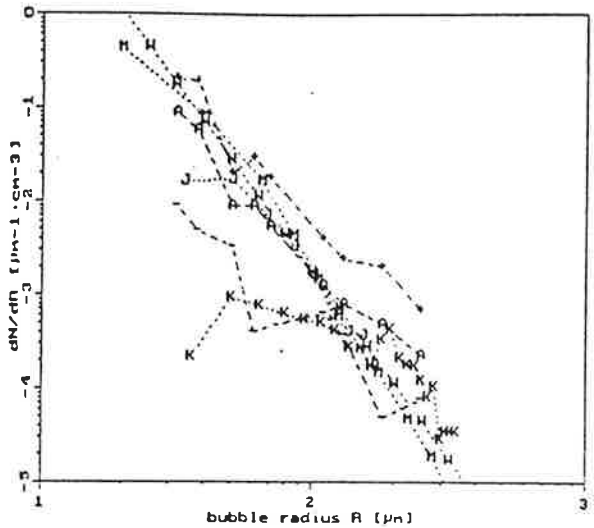

Figure 2. Bubble spectra near the ocean surface for wind speeds around 13 m/s: +, A and - are from figure 6 in Medwin and Breitz [1989]; K and J were obtained from extrapolation of the data from Kolovayev [1976] and Johnson and Cooke [1979]; M is from Monahan [1988]; W is from Wu [1989], adjusted to spectrum J.

Medwin and Breitz [1989] measured at 0.25 m below the ocean surface. Both the maximum values, measured immediately after a spilling breaker, the mean values which include breakers, and the minimum values are plotted. For radii between 50 and 100 μm, the average values compare favourably with the extrapolated Johnson and Cooke data. The discrepancy at smaller sizes is a common feature of photographic methods. For larger sizes the concentrations measured by Medwin and Breitz are higher. This may be due to understimation of the concentrations of the greater bubbles by the extrapolation method, caused by their limited penetration depths.

The bubble spectrum derived by Monahan [1988] assumes the production of only one jet droplet (J=1) and bubble rise times v_r for dirty bubbles. The slope of this spectrum is similar to the slopes of the other spectra presented in Monahan [1988] which were obtained for different values of J and v_r. Monahan's spectra have a much steeper size dependence, for bubbles greater than about 70 μm, than the other spectra shown in Figure 2. This is a consequence of the lower production rates for large particles as predicted by the Monahan et al. [1986] aerosol source function, cf. Figure 3.

The difference between the maximum and the minimum bubble concentrations from Medwin and Breitz reflects the variation in the surface bubble flux, and thus the surface aerosol source function, over the ocean surface: more than one order of magnitude.

Specific data on the variation of the bubble spectra with wave phase were obtained in the laboratory by Baldy and Bourguel [1987] from conditional sampling with an optical technique, to measure bubble spectra in the wave crest and the wave trough regions of breaking fresh water waves in the IMST tunnel. The data presented by these authors show distinct differences between both types of spectra. The concentrations increase exponentially by 4 orders

of magnitude when the depth is varied from -0.05 m (trough) to +0.06 m (crest), while also the spectral shape changes drastically. At the crest levels the concentrations decrease approximately as $r^{-1.8}$ and below the troughs as r^{-4}, with a gradual transition in between. Consequently, also the bubble-mediated aerosol production will vary strongly with wave phase.

The field observations by Medwin and Breitz [1989] and the laboratory experiments by Baldy and Bourguel [1987] indicate that the bubble concentrations near the surface reach a maximum immediately after wave breaking. The surface manifestations of the oceanic bubble spectra are the whitecaps. Oceanic whitecaps evolve through several stages during which the bubble spectrum varies as well [Monahan, 1988]. Hence also the bubble flux near the surface changes and thus also the aerosol flux at the interface. During a sequence of breaking wave events the surface production rate has an intermittent character and in high wind speeds the waves break before the effect of the previous breaker has faded. This is clearly observed from time-dependent acoustic measurements of bubble populations [Thorpe, 1982] which show the occurrence of breaks in the bubble spectra at low wind speeds, whereas at higher wind speeds continuous bubble clouds are observed.

3.2 Bubble-mediated aerosol production

The surface source function can in principle be determined from the variation of whitecap coverage with atmospheric parameters, the evolution of the bubble spectra, the bubble rise speed and the relation between bubble size and the number and size of the droplets produced per bubble. Comprehensive studies have been made of the relation between whitecap coverage and wind speed, atmospheric stability and sea water temperature [Monahan, 1983]. The time constant for exponential decay of whitecaps has been determined as 4.27 s [Monahan, 1988]. This time constant applies to the initial stage whitecap. In the later stages the bubble spectra consist predominantly of smaller bubbles which rise slower. The spectra narrow due to the smaller penetration depth of the larger bubbles and their rapid disappearance due to fast rise times, and due to dissolution of small bubbles.

Bubble-mediated aerosol production has extensively been studied, see Blanchard [1983] for a review. The number of jet droplets produced per bubble decreases exponentially with increasing bubble size. Based on data presented in Blanchard [1963, 1983], Monahan [1988] determined a relation between the jet droplet size r and parent bubble size R: $r=8.77\ 10^{-2}R+0.98$, and Wu [1989] gives an expression for the relation between the number J of jet droplets produced per bubble and the parent bubble radius: $J=7\ \exp(-2R/3)$. Film droplets are mainly produced from larger bubbles, in the range of 10-1000 from a 3 mm bubble. Bubbles smaller than 150 μm do not produce film droplets. The film droplet spectrum peaks at about 2.5 μm radius with a long tail extending beyond 15 μm, and radii <1 μm at the small end [Blanchard, 1983]. Based on Woolf et al. [1987] a jet droplet / film droplet partition function has been derived [Monahan, 1988]: $P=1-e^{-0.343r}=1-e^{-0.030R}$. Since the purpose of this paper is to explain profiles of droplets larger than about 7 μm in radius, with the application in mind to determine the influence of these large droplets on the atmospheric water vapour balance, only jet droplets are considered here.

The aerosol production rate right at the surface dF_N/dr , i.e the numberflux per radius increment per unit area per second, can be derived from the bubble size distributions as: $dF_N/dr = dN/dR \; v \; J$, where v is the terminal bubble rise speed [Thorpe, 1982] and dN/dR the number of bubbles per radius increment per unit volume. In Figure 3 we present source functions derived from the maximum and average bubble spectra observed by Medwin and Breitz [1988] (see Figure 2). The maximum bubble spectra and aerosol source functions apply to the situation immediately after wave breaking. For this situation two curves are given. The upper one (+) was obtained with rise speeds that apply to 'dirty' bubbles [Thorpe, 1982] and J=7 exp(-2R/3), which is the highest possible jet droplet flux immediately after wave breaking, in the conditions that apply to the measurements of Medwin and Breitz [1989]. The lower curve (-) was derived using the rise speeds that apply to 'dirty' bubbles and J=1. The flux indicated with A was obtained from Medwin and Breitz' average bubble spectrum using 'dirty' bubble rise speeds and J=5.

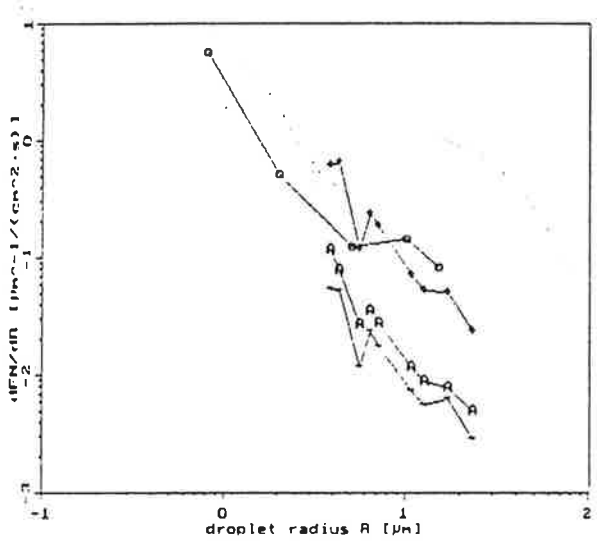

Figure 3. Aerosol source functions for wind speed 13 m/s: +, A and - were derived from Medwin and Breitz [1989] bubble spectra, see text; o is the Miller and Fairall [1988] consensus source function; the dotted lines are Monahan et al. [1988] source functions with and without spume droplets.

4. DISCUSSION

The aerosol source functions derived from the bubble spectra from Medwin and Breitz [1989] apply to the average conditions in a field of spilling breakers (curve A in Figure 3) at wind speeds of 12-15 m/s. The minimum and maximum jet droplet fluxes immediately after wave breaking indicate that the error in such estimates may be large. The influence of the rise speed is factor of 1.4 to 1.65 for the bubble size under consideration [Thorpe, 1982], so most of the uncertainty comes from the number of jet droplets per bubble. These are well known from the comprehensive studies by Blanchard [1963, 1983], but the ejection heights for the last droplets are so low that the probability to remain airborne is practically nil (because the turbulence intensity also decreases toward the surface). The ejection height decreases with water temperature [Blanchard, 1983]. Another assumption we made is that the size of

all jet droplets resulting from one bubble are equal and uniquely related to the bubble size.

All these assumptions are based on studies of single bubbles. In a whitecap the bubbles may influence each other resulting in different jet droplet production characteristics. This is one of the subjects of the PCL3 and PCL4 experiments, where bubble spectra and droplet fluxes were measured at exactly the same position over the simulated whitecap just above and just below the surface. The results are not yet available.

For practical applications, we propose to use J=5 (which is also used by Cipriano and Blanchard [1981] as well as by others) and 'dirty' bubble rise times to derive the aerosol source function from bubble spectra. This yields a source function immediately after wave breaking which is about a factor of 2 smaller than the one indicated with + in Figure 3. The maximum source function thus derived yields fluxes for droplets smaller than 10 μm that are similar to those obtained from the Miller and Fairall [1988] consensus source function at 13 m/s wind speed, but the slope in the bubble-derived source function is greater. The discrepancy may be caused by neglecting the influence of film droplets and the production of spume droplets. The contribution of film droplets can be estimated using the partition function based on Woolf et al. [1987] (see section 3.2). Both film droplets and spume droplets obviously contribute to the total concentration of the aerosol in the MABL, and is thus also taken into account by the analysis of Miller and Fairall [1988]. Comparison with the spume droplet source function proposed by Monahan et al. [1986] shows that the radius at which the spume droplets contribute is similar, but that the estimated fluxes are much lower than those proposed by Monahan et al. [1986].

The above discussion applies to the droplet source function derived from the maximum bubble spectrum obtained by Medwin and Breitz, i.e. immediately after wave breaking, while the Miller and Fairall [1988] source function is an effective one derived from aerosol concentrations in a well-mixed boundary layer. The average bubble-derived source function yields appreciably lower fluxes.

The true aerosol surface flux over the ocean must vary in time. The maximum surface flux will occur immediately after wave breaking and decay with the characteristic decay time of the surface bubble flux (which is likely size-dependent) until the next wave breaks. For estimates of the effects of sea spray on atmospheric parameters it is advised to use this time-dependent source function, with a correction for the effect of spume droplets which is still to be determined. For mixed-layer applications an effective, i.e. average, source function can be used.

The application of a time dependent source function to surface layer aerosol profiles will result in a time-dependent profile which must be added to the profile due to the 'infinite' mixed-layer reservoir. The time-average of these profiles will have much smaller gradients toward the sea surface than the profiles based on a continuous steady surface source function.

ACKNOWLEDGEMENT

I thank Bert Neger for his help with the analysis of the bubble spectra and preparing the plots. The work presented in this paper was supported by ONR, Grant N00014-87-J-1212. The author participated in the Petit-CLUSE experiments while he held a National Research Council Research Asociateship at the Naval Postgraduate School, Monterey, CA.

REFERENCES

Baldy, S., and M. Bourguel, 1987. *J. Geophys. Res.* 92, 2919-2929.
Blanchard, D.C., 1963. *Prog. Oceanog.* 1, 71-202.
Blanchard, D.C., 1983. In: P.S. Liss and W.G.N. Slinn (Eds.) *Air-sea exchange of gases and particles*, 407-454. Reidel.
Blanchard, D.C., and A.H. Woodcock, 1980. *Annals N.Y. Acad. Sci.* 338, 330-347.
Cipriano, R.J., and D.C. Blanchard, 1981. *J. Geophys. Res.* 86, 8085-8092.
De Leeuw, G., 1986. *Tellus* 38B, 51-61.
De Leeuw, G., 1987. *J. Geophys. Res.* 92, 14631-14635.
De Leeuw, G., 1988. In: Monahan and Van Patten (Eds.), *Climate and health implications of bubble-mediated sea-air exchange*, 65-82. Conn. Sea Grant College Program, CT-SG-89-06.
De Leeuw, G., 1989. *J. Geophys. Res.* 94, 3261-3269.
De Leeuw, G., 1990a. Accepted for publ. in *Tellus*.
De Leeuw, G., 1990b. Accepted for publ.in *J. Geophys. Res.*
De Leeuw et al., 1990. *Rev. Sci. Instrum.* 61, 732-735.
Edson, J.B., 1989. PhD Thesis, Penn. State Univ.
Edson, J.B., and G. de Leeuw, 1990. This proceedings volume.
Fairall, C.W. and K.L. Davidson, 1986. In: E.C. Monahan and G. MacNiocaill (Eds.), *Oceanic Whitecaps*, 195-208, Reidel.
Fairall, C.W., K.L. Davidson and G.E. Schacher, 1983. *Tellus* 35B, 31-39.
Gathman, S.G., 1989. NRL Report 9200, Washington D.C.
Johnson, B.D., and R.C. Cooke, 1979. *J. Geophys. Res.* 84, 3761-3766.
Kolovayev, P.A., 1976. *Oceanology* (Engl. Transl.) 15, 659-661.
Larsen, S.E., J.B. Edson, C.W. Fairall, G. de Leeuw and P.G. Mestayer, 1990. AMS Symp. on the role of the oceans as source and sink of trace substances that influence global change, Feb. 7-8, Anaheim, CA.
Medwin, H. and N.D. Breitz, 1989. *J. Geophys. Res.* 94, 12751-12759.
Mestayer, P.G., and Lefauconnier, 1987. *J. Geophys. Res.* 93, 572-586.
Mestayer, P.G., J.B. Edson, C.W. Fairall, S.E. Larsen, and D.E. Spiel, 1987. *Turbulent Shear Flows* 6, Springer-Verlag.
Miller, M.A., and C.W. Fairall, 1988. 7th Conf. on Ocean-Atmos. Int., Anaheim, CA, Jan. 31- Feb. 5, Am. Meteor. Soc. 174-177.
Monahan, E.C., 1988. 7th Conf. on Ocean-Atmos. Int., Anaheim, CA, Jan. 31-Feb. 5, Am. Meteor. Soc. 178-181.
Monahan, E.C., D.E. Spiel and K.L. Davidson, 1983. In: E.C. Monahan and G. MacNiocaill (Eds.), *Oceanic Whitecaps*, 167-174, Reidel.
Monahan, E.C., 1988. In: Monahan and Van Patten (Eds.), *Climate and health implications of bubble-mediated sea-air exchange*, 43-63. Conn. Sea Grant College Program, CT-SG-89-06.
Monahan, E.C., 1983. In: P.S. Liss and W.G.N. Slinn (Eds.) *Air-sea exchange of gases and particles*, 129-163. Reidel.
Rouault, M., P.G. Mestayer and R. Schiestel, 1990. In preparation.

Stramska, M., 1987. *Acta Geophysica Polonica* 35, 87-100.
Thorpe, S.A., 1982. *Phil. Trans. R. Soc. Lond.* A304, 155-210.
Toba, Y., 1965. *Tellus* 17, 131-145.
Woodcock, A.H., 1953. *J. Meteorol.* 10, 362-371.
Woolf, D.K., P.A. Bowyer and E.C. Monahan, 1987. *J. Geophys. Res.* 92, 5142-5150.
Wu, J., 1981. *J. Geophys. Res.* 86, 457-463.
Wu, J., 1988. *J. Geophys. Res.* 93, 587-590.
Wu, J., 1989. *Tellus* 41B, 469-473.
Wu, J., 1990. Accepted for publication in *J. Geophys. Res.*
Wu J., J.J. Murray and R.J. Lai, 1984. *J. Geophys. Res.* 89, 8163-8169.

Modelling the Fate and Influence of Marine Spray

Proceedings of a workshop held 6-8 June 1990, Luminy, Marseille, France

Patrice G. Mestayer, Edward C. Monahan, and Patricia A. Beetham, Editors

This workshop brings to a conclusion the international cooperative research program CLUSE - HEXIST 3, 1988-1990, sponsored by the National Science Foundation (via Grant INT-8715148) and the Centre National de la Recherche Scientifique (via Grant AI (06943)8131) under the auspices of the U.S.-France Cooperative Science Program.

CLUSE

HEXIST

HEXOS

SEA SURFACE PHYSICS LAB

MSI, UCONN AVERY POINT

WHITECAP

PROJECT

HEXOS CONTRIB. No. 24

Whitecap Report No. 7
Marine Sciences Institute
University of Connecticut
Avery Point Groton, CT 06340
June 1990